Materials Physics and Mechanics 37 (2018) 146-152 Received: December 22, 2017

MAGNETIC FIELD SENSOR FOR NON-INVASIVE CONTROL MEDICAL IMPLANTS

L.P. Ichkitidze[1,2]*, M.V. Belodedov[3], S.V. Selishchev[1], D.V. Telishev[1,2]

[1]National Research University of Electronic Technology,

bld. 1, Shokin Square, Zelenograd, Moscow, 124498, Russia

[2]I.M. Sechenov First Moscow State Medical University,

bld. 4, Bolshaya Pirogovskaya Str., 2, Moscow, 119991, Russia

[3]National Research University of Technology (BMSTU), ul. Baumanskaya, 2-ya, 5/1, Moscow, 105005 Russia

*e-mail: ichkitidze@bms.zone

Abstract. The magnetomodulation differential weak magnetic-field sensor, based on the Bi-2223 high-temperature superconducting ceramics has been investigated. The high magnetic-field resolution (~20 pT) and wide measurement range (125 – 140 dB) have been obtained. The possibility of using this sensor for noninvasive control of magnetic particles or implanted medical electronic devices in biological objects at a distance of up to 30 mm from the skin surface is discussed.

Keywords: high-temperature superconducting ceramic; magnetic-field sensor; magnetic-field resolution; noninvasive control; medical implants.

1. Introduction

Weak magnetic fields ($B \leq 10$ nT) are currently measured using different systems, including superconducting quantum interference devices (SQUIDs), combined magnetic field sensors (CMFSs), nuclear magnetic resonance laser pump magnetometers, and ferroprobe transformers (FTs) [1]. Among these systems, SQUIDs, which have been already commercially produced, have the highest sensitivity [2 – 4]. However, they are brittle, expensive, and do not detect the absolute value in the measured magnetic field.

The absolute value of magnetic field can be directly measured using FTs and CMFSs. The former, however, have serious drawbacks, specifically, the large measuring error in the weak-field range ($B \leq 1$ nT) and the narrow passband (≤ 1kHz) and dynamic measurement range $D_r \leq 60$ dB [5, 6]. The CMFSs still have been developed and tested [7 – 9], but in future their modifications containing nanosized elements can become competitive with SQUIDs [2 – 4].

A high-temperature superconducting (HTS) ceramic material investigated here consists of numerous grains with the Josephson junctions, formed between their boundaries. The magnetization curve (dependence of the magnetic flux ϕ on external field B) of such a Josephson medium is characterized by the strong nonlinearity, which increases near critical temperature T_c and was used to design the so-called magnetomodulation sensor (MMS) of weak magnetic fields ($B \leq 10$ nT). In the previous works, the MMSs were designed on the base of a Y-123 HTS ceramic material with $T_c \sim 90$ K. At a working temperature of $T \sim 77$ K (the liquid nitrogen boiling point), the $\phi(B)$ dependence of the Y-123 ceramics is strongly

http://dx.doi.org/10.18720/MPM.3722018_6

nonlinear; therefore, the sensor, fabricated from this material, is characterized by the high magnetic-field sensitivity $S = dU / dB$, where U is the response signal [10 - 13]. At the same time, the Y-123 ceramic-based sensors have certain drawbacks, e.g., the narrow measurement range ($|B| \leq 0.3$ mT), low magnetic-field resolution $\delta B \geq 50$ pT and magnetic-flux resolution $\delta\phi \geq 10\ \phi_0$ ($\phi_0 = 2.07 \times 10^{-15}$ Vb is the magnetic flux quantum), and the limited dynamic range ($D_r \leq 110$ dB). In addition, such sensors degrade in air under normal storage conditions. In contrast to the Y-123 ceramics, the Bi-2223 bismuth HTS ceramic material is stable and has $T_c \sim 105 – 108$ K [14]; therefore, MMSs based on it are expected to have the higher performances as compared with the Y-123-based sensor [12,13].

In this study, we investigate a weak magnetic-field sensor based on the Bi-2223 HTC ceramics with a working temperature of $T \sim 77$ K. The minimum size of iron magnetic grains that could be detected by the MMS under study is estimated.

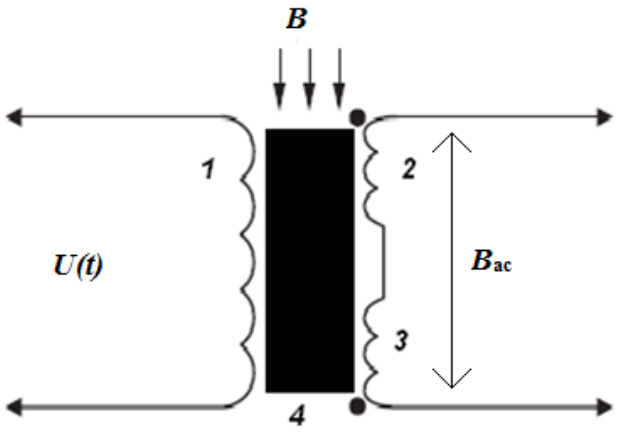

Fig. 1. Coils and core MMS: 1 – excitation coil, 2 and 3 – signal coils, connected in series and opposite to each other, 4 – cylindrical core of ceramic Bi-2223. The measured B is directed parallel to the z-axis, $U(t)$ is the registered variable signal.

2. Experimental

The main MMS element, i.e., a magnetic-field sensitive cylindrical rod, was fabricated from the Bi-2223 ceramic powder, which was tableted and annealed in accordance with the well-developed ceramic technology [14]. Cylindrical rods with a length of 18 – 20 mm and a dimeter of ~ 4 mm were cut from the prepared tablets. Two coils were tightly wound over almost the entire sample length (~16 mm); the exciting coil, consisting of two identical back-to-back sections each, containing 200 turns, was covered by a signal coil, containing 400 turns. The back-to-back identical halves of the exciting coil ensure operation of the investigated MMS in the differential regime, which automatically eliminates the effect of odd response harmonics on the signal winding. A superconducting cylindrical rod (sensor core) was positioned vertically along the z-axis; the x and y directions lied in the horizontal plane (Fig. 1).

All the measurements were performed in the geometry with the measured magnetic field $\vec{B}$ parallel to the z-axis of the cylindrical rod. Only the z projections of the background Earth's magnetic field B_b were taken into account, since the other two projections (x and y) of this field did not significantly affect the characteristics of the investigated MMS. The MMS

was mounted in a nitrogen cryostat so that the distance of the near sensor end to the outer cryostat surface was no larger than $d \sim 6 – 7$ mm.

The sensor rod had the low critical current density (≤ 10 A/cm^2) and $T_c \approx 105$ K. The measured weak dc magnetic field $\vec{B}$ was induced by the Helmholtz coils. All the measurements were performed at $T \sim 77$ K (liquid nitrogen temperature). The directions of field $\vec{B}$ and exciting magnetic field $\vec{B}_{ac}$ were collinear: $\vec{B} \| \vec{B}_{ac}$. The ac magnetic field was sinusoidal: $B_{ac} = B_m \sin(\omega t)$, where B_m is the amplitude, $\omega = 2\pi f$ is the cyclic frequency, f is the frequency, and t is the time. Sometimes, the field B_b was compensated to a level of ~1μT using the Helmholtz coils. The response signal U was detected by a selective nanovoltmeter with a selectivity of 40 dB/octave.

Figure 2 shows signals of the $U(t)$ response of the MMS to the exciting ac magnetic field with a frequency of f =10 kHz and an amplitude of $2B_m$ =1000 μT (peak–peak). The $U(f)$ dependences were recorded upon continuous variation in the frequency f. To exclude the sensor nonlinearity unrelated to its superconducting properties, the response was measured at room temperature $T \approx 300$ K (Fig. 2a).

It can be seen that in the normal state, all harmonics, except for the first one, are missing, which confirms the absence of unexpected nonlinearity of the sensor, which can be caused, e.g., by ferromagnetic parts of the sensor.

It follows from Figs. 2b and 2c that at $B_b \approx 1$ μT, the response contains only odd harmonics, while at $B_b \approx 50$ μT, all the harmonics are observed at T = 77 K. Such a behavior is typical of HTS ceramic materials and emphasizes their magnetic-field sensitivity. The higher harmonic amplitude decreased with increasing f and under voltages of ≤ 0.01 mV, the harmonics higher than the seventh order were not observed.

3. Results

Figure 3 shows a typical dependence of the second-harmonic amplitude U_2 on the applied dc magnetic field B.

It can be seen that the $U_2(B)$ dependence shifts along the horizontal axis by $B_b \sim 50$ μT (background Earth's magnetic field) and has the maxima at $B^* \sim \pm 700$ μT. The highest magnetic-field sensitivity $S_U = dU_2 / dB$ is attained in weak fields ($B \approx 0$). As the B value increases, S_U gradually decreases and at $B = B^*$ approaches the zero value. Thus, using the quasi-linear $U_2(B)$ dependence in weak fields $0 < B < 700$ μT, a high-sensitivity MMS can be designed on the basis of the Bi-2223 ceramics. It is worth noting that when the background Earth's magnetic field is compensated, i.e., at $B_b \leq 1$ μT, the S_U value additionally increases by more than 10%.

In the range of $|B| \leq 20$ μT, the $U_2(B)$ dependences are linear and the S_U value increases linearly with f. Indeed, it follows from Fig. 4 that S_U increases by a factor of 7.4 with a sevenfold increase in f.

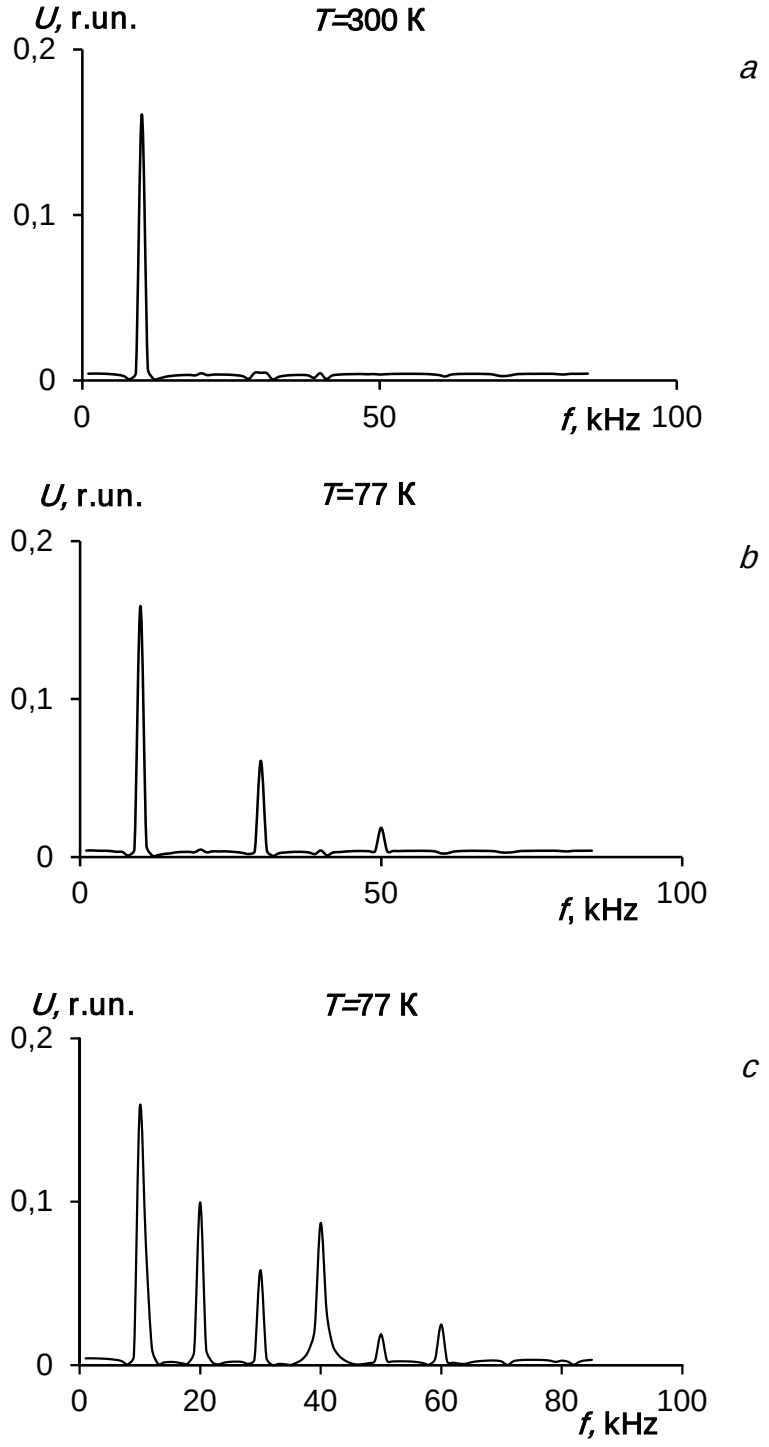

Fig. 2. Response U (relative units) of the sensor with f = 10 kHz and $2B_m$ =1000 μT (peak–peak) under different conditions: (*a*) T = 300 K, $B_b \approx 1$ μT; (*b*) T = 77 K, $B_b \approx 1$ μT; (*c*) T = 77 K, $B_b \approx 50$ μT.

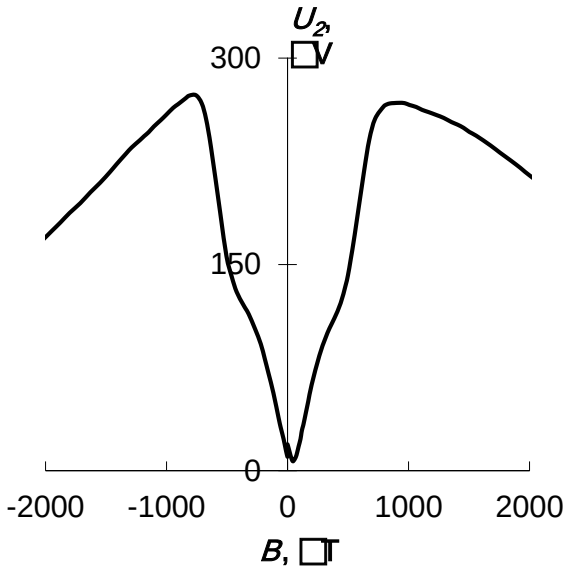

Fig. 3. Dependence $U_2(B)$ at f = 10 kHz and $2B_m$ = 600 μT (peak-peak). The background magnetic field of the Earth is uncompensated.

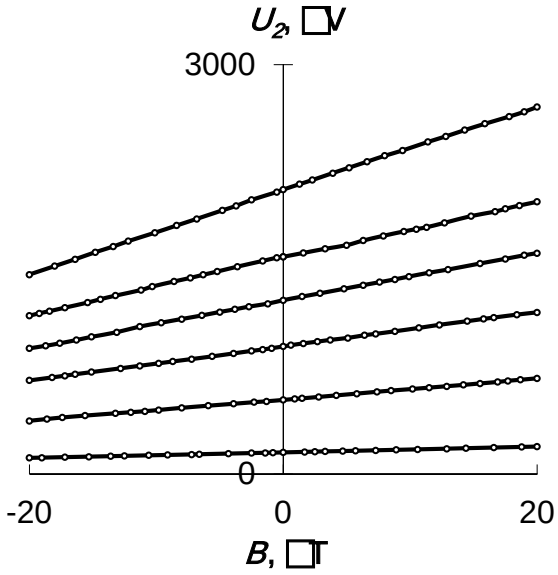

Fig. 4. Dependence $U_2(B)$ at $2B_m$ = 1000 μT (peak-peak) and various f, kHz (bottom-up): 5; 10; 15; 20; 25; 35. The background magnetic field of the Earth is uncompensated.

4. Discussion

The dependence of magnetic flux ϕ on field B in a superconducting rod is an odd nonlinear function and can be expressed in the first approximation as

$$\phi = A_0\left(k_1 B - k_3 B^3 - k_5 B^5\right), \tag{1}$$

where A_0 is the rod cross-sectional area and k_1, k_3, and k_5 are the coefficients.

In Equation (1), it is necessary to take into account all the investigated magnetic fields B, B_{ac}, and B_b in both halves of the exciting coil. Then, the ϕ value is

$$\phi = A_0\left[\left(k_{11}\left(B + B_b + B_{ac}\right) - k_{31}\left(B + B_b + B_{ac}\right)^3 - k_{51}\left(B + B_b + B_{ac}\right)^5\right) + \right.$$
$$\left. + \left(k_{12}\left(B + B_b - B_{ac}\right) - k_{32}\left(B + B_b - B_{ac}\right)^3 - k_{52}\left(B + B_b - B_{ac}\right)^5\right)\right], \tag{2}$$

where k_{11}, k_{12}, k_{31}, k_{32} , k_{51}, and k_{52} are the coefficients, characterizing the first and second coil halves, respectively. In Equation (2), only the z projections of the magnetic fields are taken into account, since the other projections are negligible.

The signal, induced in the receiving coil, consisting of n turns is

$$U = -n\frac{d\phi}{dt}. \tag{3}$$

According to (1) – (3), the signal response at the second harmonic is

$$U_2 \approx An\omega B_m^2\left[12k_{30}\left(B + B_b\right) + 20k_{50}\left(B + B_b\right)^3 + 10k_{50}\left(B + B_b\right)B_m^2\right]\sin\left(2\omega t\right) + u_2, \tag{4}$$

where u_2 is the unbalance signal and A is the average cross-sectional area of the signal coil. In Equation (4), we made the designations:

$$k_{30} = \frac{k_{31} + k_{32}}{2}; \quad k_{50} = \frac{k_{51} + k_{52}}{2}; \quad \Delta k_{10} = k_{11} - k_{12}. \tag{5}$$

The u_2 value tends to zero with a decrease in the difference between two halves of the core, i.e., when the quantities Δk_{10}, $\Delta k_{30} = k_{31} - k_{32}$, and $\Delta k_{50} = k_{51} - k_{52}$ turn to zero.

The thorough analysis of Equation (4) showed that at $B_b >> B$, $\Delta k_{50}/k_{50} \geq 1\%$, and $\Delta k_{30}/k_{30} \geq 1\%$, and a nanovolmeter selectivity of ~40 dB/octave, the u_2 value approaches the response at the second harmonic, which leads to a decrease in the magnetic-field sensitivity S_U. In the opposite situation, i.e., at $B_b \approx 0$, the u_2 value is minimum and the S_U value is maximum. This conclusion explains the obtained experimental result, i.e., the S_U growth after compensation of B_b.

According to Fig. 3, we have $S_U \sim 50$ V/T at $f \approx 35$ kHz and $B_b \approx 50$ μT. Taking into account the minimum detected signal level $\delta U_2 \sim 0.001$ μV, we obtain the minimum detected field $\delta B \approx \delta U_2 / S_U \sim 20$ pT. This value is not limited by the internal magnetic noise level $\delta B \leq 1$ pT of the Bi-2223 HTS ceramic material [15]. Hence, the magnetic-field sensitivity of the investigated MMS can be further enhanced.

The dynamic measurement range at $|B| \approx 20$ μT and $\delta B \sim 20$ pT is $D_r \sim 125$ dB and, in the case of $\delta B \sim 1$ pT, it is $D_r \sim 150$ dB. The total measurement range at $|B| \approx 600$ μT and $\delta B \sim 50$ pT is very wide and attains 140 dB.

The MMS is a differential sensor, the magnetic-field sensitivity of which can be increased in two ways: via increasing the ω, k_{30}, k_{50}, and B_m values or decreasing the external magnetic fields, including industrial noise and background Earth's magnetic field, and the Δk_{10}, Δk_{30}, and Δk_{50} values. For example, according to Equation (4), with an increase in the frequency f from 35 to 500 kHz, the $U_2(B)$ and S_U values grow proportionally; therefore, the δB value decreases to $\delta B \sim 1$ pT. In this case, the increase in the reactive resistance to a level of 1 Ω cannot significantly affect the MMS characteristics.

Thus, the magnetomodulation sensor, based on the Bi-2223 HTC ceramic material, exhibits a magnetic-field resolution of $\delta B \sim 20$ pT, which can be reduced to a level of 1 pT or lower.

Modern medical implants, sensors, and biocompatible materials often contain electronic components and conducting or magnetic particles. In particular, the implanted coils are used for wireless energy supply to various electrical implants, stimulators, artificial blood circulatory systems, etc. [16, 17], or carbon nanotubes and nanomaterials, based on them, containing catalytic magnetic particles [18, 19]. Detection of their magnetic fields will open the way to the noninvasive control of their operation.

The estimations made here showed that the investigated MMS with $\delta B \sim 20$ pT can detect weak magnetic fields of spherical magnetic particles ~100 μT in diameter at a distance of 10 mm from the sensor. At $\delta B \sim 1$ pT, the same particles can be detected at a distance of 25 – 30 mm from the near MMS end. In addition, magnetic particles, located under skin at a depth of 4 – 20 mm, can be detected ($d \sim 6 - 7$ mm). These estimations are apparently valid for various implants, located at a depth of up to 20 mm under the skin.

5. Conclusions

The investigated differential weak magnetic-field magnetomodulation sensor, based on the Bi-2223 HTC ceramic material, has a number of parameters typical of ferroprobe transformers, including the possibility of measuring the absolute value of the magnetic field,

simple design and fabrication, high magnetic-field sensitivity, and an accompanying electronic system. The sensor has the benefits of HTS SQUIDs, i.e., the high magnetic-field sensitivity and magnetic-field resolution (~ 20 pT) and wide measurement range (125 – 140 dB). The design simplicity and stability against degradation are certain advantages of the proposed sensor over the HTS SQUIDs.

These magnetometers can compete with the HTS SQUID magnetometers in, e.g., biomedical applications, such as noninvasive control of magnetic particles or various medical implants in biological objects.

Acknowledgement. *This work was provided by the Ministry of Education and Science of the Russian Federation (Grant 20.9216.2017/6.7).*

References

[1] D. Robbes // *Sensors and Actuators A: Physical* **129(1)** (2006) 86.
[2] www.tristantech.com
[3] www.starcryo.com
[4] www.supracon.com
[5] L. Jian // *Measurement* **46** (2013) 710.
[6] L. Jian // *Measurement Science Review* **12(6)** (2012) 286.
[7] M. Pannetier-Lecoeur, L. Pakkonen, N. Sergeeva-Chollet et al. // *Applied Physics Letters* **98(15)** (2011) 153705.
[8] L.P. Ichkitidze, A.N. Mironyuk // *Physica C: Superconductivity* **472(1)** (2012) 57.
[9] L.P. Ichkitidze // *AIP Advances* **3(6)** (2013) 062125.
[10] C.M. Wilson, G. Johansson, A. Pourkabirian et al. // *Nature* **479(7373)** (2011) 376.
[11] A.I. Golovashkin, N.D. Kuzmichev, V.V. Slavkin // *Technical Physics. The Russian Journal of Applied Physics* **53(10)** (2008) 1314.
[12] M.V. Belodedov, S.V. Chernih // *Instrum. and Experimen. Techniques* **44(4)** (2001) 568.
[13] V.K. Ignatev, S.V. Chernih // *Instrum. and Experimen. Techniques* **39(2)** (1996) 272.
[14] Y.E. Grigorashvily, L.P. Ichkitidze, N.N. Volik // *Physica C* **435** (2006) 140.
[15] B. David, D. Grundler, S. Krey et al. // *Supercond. Sci. Technol.* **9** (1996) A96.
[16] A.A. Danilov, E.A. Mindubaev, S.V. Selishchev // *Progress in Electromagnetics Research B* **69(1)** (2016) 61.
[17] A.A. Danilov, E.A. Mindubaev, S.V. Selishchev // *Progress in Electromagnetics Research M* **44** (2015) 91.
[18] L.P. Ichkitidze, V.M. Podgaetski, O.V. Ponomareva et al. // *Izvestia VUZov. Physika* **53(3-2)** (2010) 125 (In Russian).
[19] L.P. Ichkitidze, V.M. Podgaetski, A.S. Prihodko et al. // *Biomedical Engineering* **47** (2013) 68.